Crystal Structures of Phosphodiesterases 4 and 5 in Complex with Inhibitor 3-Isobutyl-1-methylxanthine Suggest a Conformation Determinant of Inhibitor Selectivity*

Qing Huai‡, Yudong Liu‡, Sharron H. Francis§, Jackie D. Corbin§, and Hengming Ke‡¶

*From the ‡Department of Biochemistry and Biophysics and Lineberger Comprehensive Cancer Center,
the University of North Carolina, Chapel Hill, North Carolina 27599-7260 and the §Department of Molecular
Physiology and Biophysics, Vanderbilt University School of Medicine, Nashville, Tennessee 37232-0615*

Cyclic nucleotide phosphodiesterases (PDEs) are a superfamily of enzymes controlling cellular concentrations of the second messengers cAMP and cGMP. Crystal structures of the catalytic domains of cGMP-specific PDE5A1 and cAMP-specific PDE4D2 in complex with the nonselective inhibitor 3-isobutyl-1-methylxanthine have been determined at medium resolution. The catalytic domain of PDE5A1 has the same topological folding as that of PDE4D2, but three regions show different tertiary structures, including residues 79–113, 208–224 (H-loop), and 341–364 (M-loop) in PDE4D2 or 535–566, 661–676, and 787–812 in PDE5A1, respectively. Because H- and M-loops are involved in binding of the selective inhibitors, the different conformations of the loops, thus the distinct shapes of the active sites, will be a determinant of inhibitor selectivity in PDEs. IBMX binds to a subpocket that comprises key residues Ile-336, Phe-340, Gln-369, and Phe-372 of PDE4D2 or Val-782, Phe-786, Gln-817, and Phe-820 of PDE5A1. This subpocket may be a common site for binding nonselective inhibitors of PDEs.

Cyclic nucleotide phosphodiesterases (PDEs)[1] hydrolyze cAMP and cGMP to 5′-AMP and 5′-GMP. The second messengers, cAMP and cGMP, mediate the response of cells to a wide variety of hormones and neurotransmitters and modulate many metabolic processes such as cardiac and smooth muscle contraction, glycogenolysis, platelet aggregation, secretion, lipolysis, ion channel conductance, apoptosis, and growth control (1–6).

The human genome encodes 21 PDE genes and over 60 PDE isoforms categorized into 11 families (7–16). PDE molecules contain three regions: an N-terminal splicing region, a regulatory domain, and a catalytic domain near the C terminus. The 11 PDE families share a conserved catalytic domain of about 300 amino acids but rare homology in other regions across families. The function of the N-terminal splicing region of the PDE families is unknown. The regulatory domains of PDEs contain various structural motifs such as a calmodulin-binding domain in PDE1, upstream conserved region in PDE4, PAS (period clock protein, aryl hydrocarbon receptor nuclear translocator, and single-minded protein) domain in PDE8, GAF (cGMP-specific PDE, adenylyl cyclase, and Fh1A) domain in PDE2, -5, -6, -10, and -11. The regulatory domains have been shown to play roles in the regulation of the catalytic activity of PDEs or to participate in cross-talk with other signaling pathways (16–18).

PDEs share high degree (25–49%) of amino acid conservation in the catalytic domains, implying a similar three-dimensional structure of the catalytic domains. However, PDE families and isoforms within the respective family have varying substrate preferences for cAMP and cGMP. The PDE4, -7, and -8 families prefer to hydrolyze cAMP, whereas PDE5, -6, and -9 are cGMP-specific. PDE1, -2, -3, -10, and -11 show activities toward both substrates but have distinct K_m values for cAMP and cGMP (16). In addition, many PDE families possess selective inhibitors that bind to the conserved active site. For example, rolipram is a PDE4-selective inhibitor, and sildenafil (VIAGRA™) is a PDE5-selective inhibitor (19).

In the past 3 decades, selective inhibitors of PDEs have been widely studied as therapeutics such as cardiotonics, vasodilators, smooth muscle relaxants, antidepressants, antithrombotics, antiasthmatics, and agents for improving cognitive functions such as learning and memory (20–24). Many PDE inhibitors have been in clinical trials or have already entered the marketplace. For example, the PDE3-selective inhibitor cilostazol (Pletal™) is a drug for the reduction of symptoms of intermittent claudication, and the PDE5 inhibitors sildenafil (Viagra™), vardenafil (Levitra™), and tadalafil (Cialis™) are used for treatment of male erectile dysfunction. Selective inhibitors of PDE4 have been studied as anti-inflammatory drugs for asthma and chronic obstructive pulmonary disease (24–30).

Extensive biochemical, pharmacological, and clinical studies have been performed on PDEs and their selective inhibitors. However, the mechanisms by which the conserved active sites of PDEs recognize a common inhibitor and distinguish selective inhibitors remain mysteries. Structural studies on the catalytic domain of unligated PDE4B (31), PDE4D in complex with inhibitor zardavarine (32), PDE4D2 in complex with rolipram (33) and AMP (34), and PDE5A in complex with sildenafil (35) have provided preliminary understanding of inhibitor selectivity. Here we report the structures of the catalytic domains of human PDE5A1 and PDE4D2 in complex with a nonselective inhibitor 3-isobutyl-1-methylxanthine (IBMX). These structures reveal a common subpocket in the active site of PDEs for

The atomic coordinates and structure factors (code 1RKO and 1RKP) have been deposited in the Protein Data Bank, Research Collaboratory for Structural Bioinformatics, Rutgers University, New Brunswick, NJ (http://www.rcsb.org/).

¶ To whom correspondence should be addressed. Tel.: 919-966-2244; Fax: 919-966-2852; E-mail: hke@med.unc.edu.

[1] The abbreviations used are: PDE, phosphodiesterase; IBMX, 3-isobutyl-1-methylxanthine.
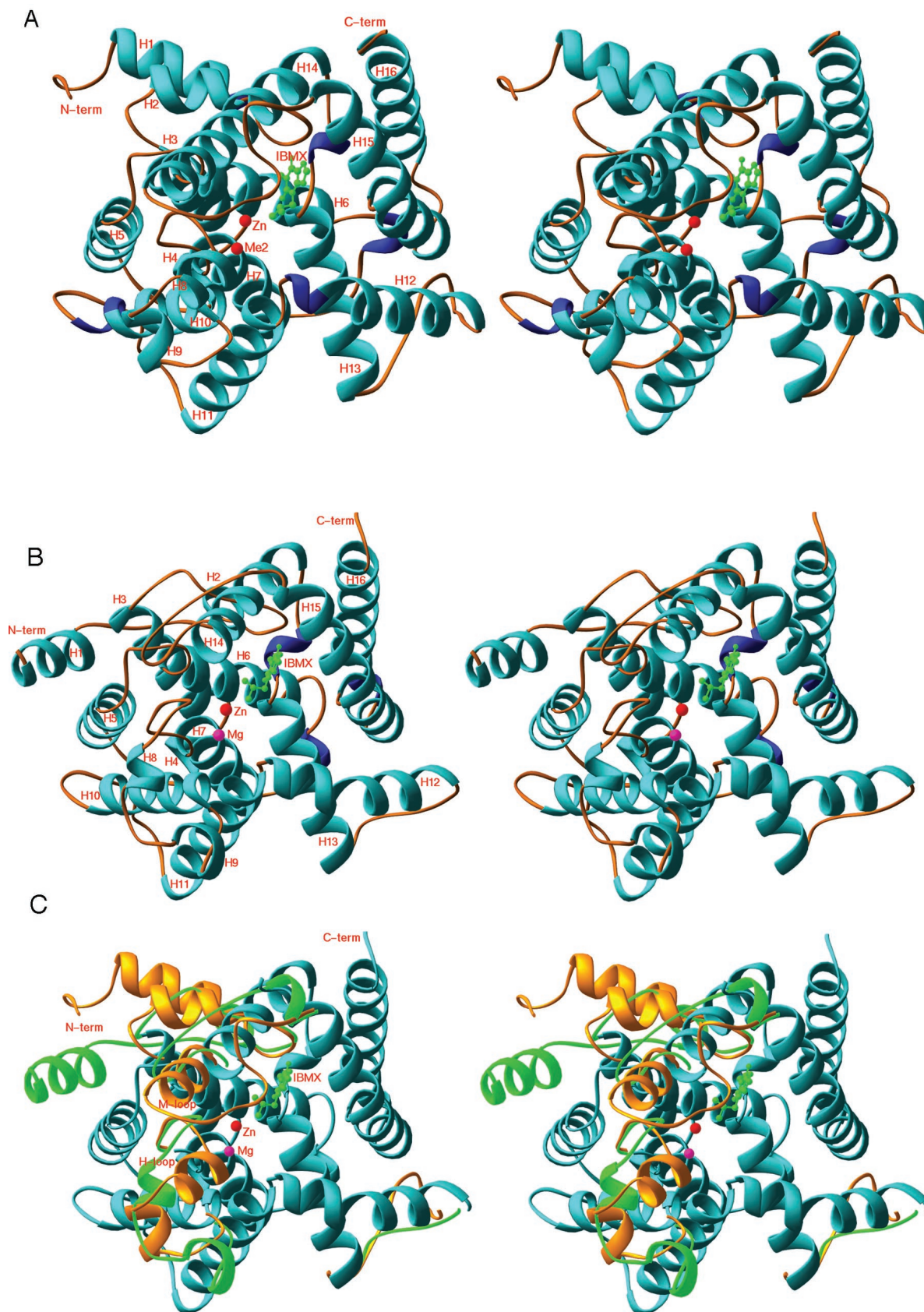
FIG. 1. **Structures of the PDE-IBMX complexes.** *A*, ribbon diagram of PDE4D2-IBMX. The α-helices are colored as *cyan*, and *blue* color represents 3_{10} helices. The first metal ion is interpreted as zinc, as discussed previously (31, 33), whereas the second metal ion (*Me2*) is ambiguous. *B*, ribbon diagram of PDE5A1-IBMX. The second metal ion was assigned as magnesium because 0.2 M MgSO$_4$ was used in the crystallization buffer. *C*, the structural superposition between PDE4D2 and PDE5A1. The *cyan ribbons* represent the conserved core structures between PDE4D2 and PDE5A1. The variable regions are drawn in *gold* for PDE4D2 and *green* for PDE5A1. *D*, the correspondence of amino acid sequence to the secondary structures.

D

```
                       H1            3₁₀              H2                    H3
pde4d2(79)   IPRFGVKTEQ EDVLAKELED VNKWGLHVFR IAELSGNRPL TVIMHTIFQE 128
pde5a1(535)  EETRELQSLAA AVVPSAQTLK ITDFSFSDFE L----SDLET ALCTIRMFTD 581
                   H1          H2                            H3

                  H4          H5                         H6
pde4d2       RDLLKTFKIP VDTLITYLMT LEDHYHADVA YHNNIHAADV VQSTHVLLST 178
pde5a1       LNLVQNFQMK HEVLCRWILS VKKNYRKNVA YHNWRHAFNT AQCMFAALKA 631
                  H4          H5                         H6

             3₁₀          H7                 H8         H9
pde4d2       PALEAVFTDL EILAAIFASA IHDVDHPGVS NQFLINTNSE LALMYNDSSV 228
pde5a1       GKIQNKLTDL EILALLIAAL SHDLDHRGVN NSYIQRSEHP LAQLY-CHSI 680
             3₁₀          H7                 H8         H9

                  H10         3₁₀             H11            3₁₀
pde4d2       LENHHLAVGF KLLQEENCDI FQNLTKKQRQ SLRKMVIDIV LATDMSKHMN 278
pde5a1       MEHHHFDQCL MILNSPGNQI LSGLSIEEYK TTLKIIKQAI LATDLALYIK 730
                  H10                        H11            H12

                  H12                    H13               3₁₀
pde4d2       LLADLKTMVE TKKVTSSGVL LLDNYSDRIQ VLQNMVHCAD LSNPTKPLQL 328
pde5a1       RRGEFFELIR ------KNQF NLEDPHQKEL FLAMLMTACD LSAITKPWPI 774
                  H12                        H13            3₁₀

                       H14                                    H15
pde4d2       YRQWTDRIME EFFRQGDRER ERGMEISP-- MCDKHNASVE KSQVGFIDYI 376
pde5a1       QQRIAELVAT EFFDQGDRER KELNIEPTDL MNREKKNKIP SMQVGFIDAI 824
                  H14                                        H15

                  H15                   H16
pde4d2       VHPLWETWAD LVHPDAQDIL DTLEDNREWY QSTIPQ 412
pde5a1       CLQLYEALTH VS-EDCFPLL DGCRKNRQKW QALAEQQ 860
                  H15                   H16
```
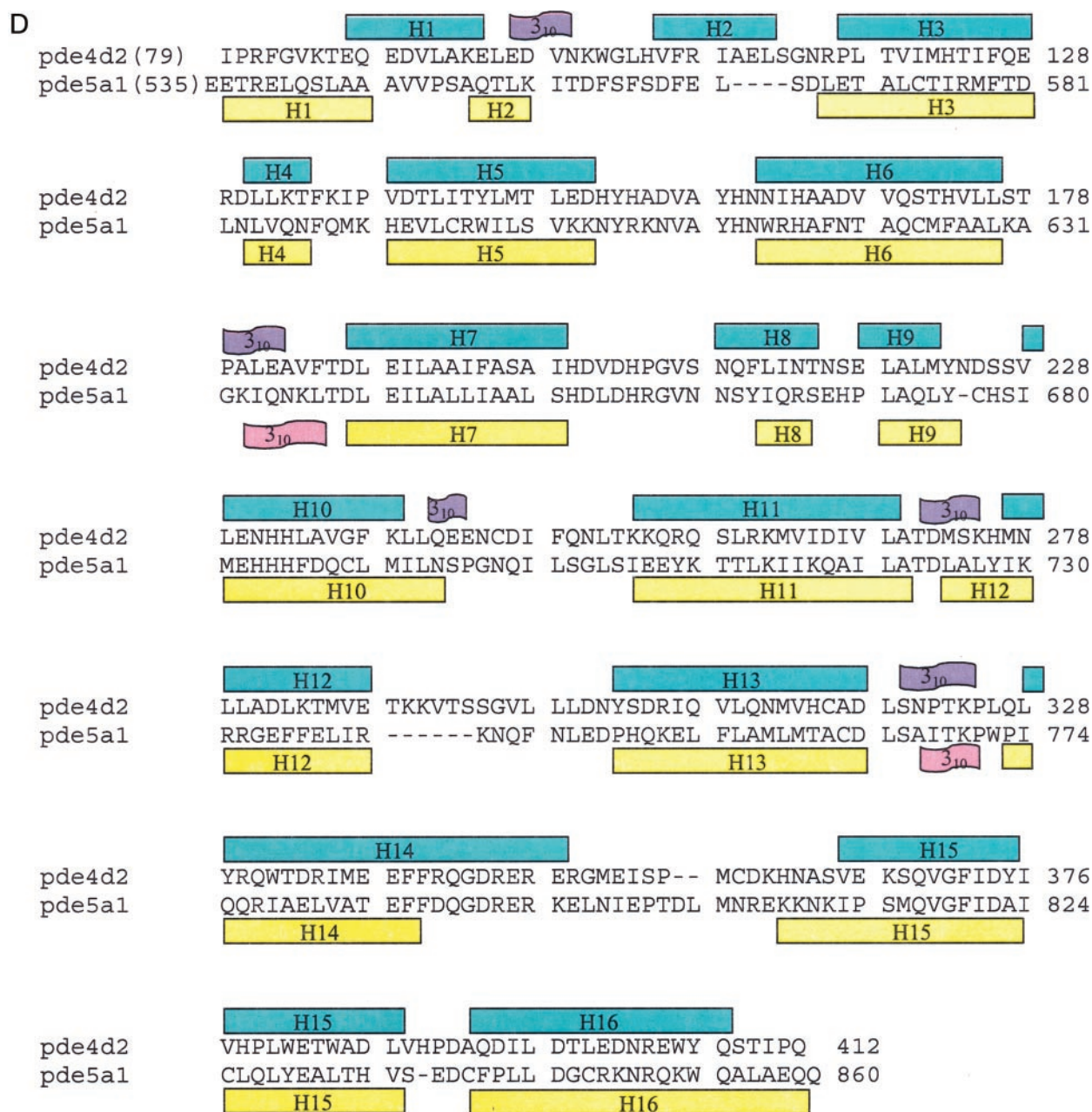
FIG. 1—*continued*

binding of this nonselective inhibitor. Structural comparison between PDE4 and PDE5 suggests that conformational difference, in addition to the specific amino acid determinants, is another mechanism of inhibitor selectivity.

EXPERIMENTAL PROCEDURES

Protein Expression and Purification—The catalytic domain of human PDE4D2 (BF059733) was expressed in *Escherichia coli* and purified as described previously (33). The cDNA of the catalytic domain of human *PDE5A1* was generated by site-directed mutagenesis of the bovine *PDE5A1* gene. The coding regions for amino acids 535–860 of *PDE5A1* were amplified by PCR and subcloned into the expression vector pET15b. The resultant plasmid pET-PDE5A1 was transformed into *E. coli* strain BL21 (Codonplus) for overexpression. The *E. coli* cell carrying pET-PDE5A1 was grown in LB medium at 37 °C to $A_{600} = 0.7$, and then 0.1 mM isopropyl β-D-thiogalactopyranoside was added for further growth at 15 °C overnight. Recombinant PDE5A1 was purified by nickel-nitrilotriacetic acid affinity column (Qiagen), thrombin cleavage, Q-Sepharose (Amersham Biosciences), and Sephacryl S300 (Amersham Biosciences) columns. The PDE5A1 protein had purity greater than 95% as shown by SDS-PAGE. A typical batch of purification yielded over 10 mg of PDE5A1 from a 2-liter cell culture. The fragment of human PDE5A1 expressed in *E. coli* had a catalytic activity of about 2 μmol/min/mg, which is comparable with that of the protein expressed in a baculovirus system (36).

Crystallization and Data Collection—Crystals of PDE4D2-IBMX and PDE5A1-IBMX were grown by hanging drop. The catalytic domain of 15 mg/ml PDE4D2 (amino acids 79–438) in a storage buffer of 50 mM NaCl, 20 mM Tris·HCl (pH 7.5), 1 mM β-mercaptoethanol, and 1 mM EDTA was mixed with 5 mM IBMX. The PDE4D2-IBMX complex was crystallized against a well buffer of 0.1 M HEPES (pH 7.5), 20% PEG3350, 30% ethylene glycol, 10% isopropyl alcohol, and 5% glycerol at 4 °C. The well buffer was used as the cryosolvent for freezing the crystals in liquid nitrogen. Diffraction data were collected on beamline 14C at Advanced Photon Source (Table I). The PDE4D2-IBMX crystal has the space group P2₁2₁2₁ with cell dimensions of $a = 99.3$, $b = 112.5$, and $c = 160.9$ Å. The catalytic domain of 10 mg/ml PDE5A1 (amino acids 535–860) was mixed with 5 mM IBMX and crystallized against a well buffer of 0.1 M Tris·base (pH 7.5), 17% PEG3350, and 0.2 M MgSO₄ at room temperature. To freeze the crystals in liquid nitrogen, the

TABLE I
Statistics on diffraction data and structure refinement

	Data collection PDE5A1-IBMX	PDE4D2-IBMX
Space group	P3$_1$21	P2$_1$2$_1$2$_1$
Unit cell (*a, b, c*, Å)	74.5, 74.5, 130.1	99.7, 111.7, 159.4
Resolution (Å)	2.05	2.1
Total measurements	211,071	754,083
Unique reflections	27,018	94,246
Completeness (%)	100.0 (100.0)[a]	91.0 (64.4)[a]
Average I/σ	13.4 (4.9)[a]	18.9 (3.3)[a]
R_{merge}	0.063 (0.475)	0.074 (0.440)[a]
Structure refinement		
R-factor	0.220	0.226
R-free	0.243	0.259
Resolution (Å)	50–2.05	50–2.1
Reflections	25,797	89,970
r.m.s.d.[b] for bond	0.0059 Å	0.0059
r.m.s.d. for angle	1.20°	1.09°
Average B-factor (Å^2)		
All atoms	36.6 (2674)[c]	32.8 (10,987)
Protein	36.6 (2541)	32.8 (10,726)
IBMX	27.5 (16)	58.9 (64)
Waters	35.1 (133)	27.8 (189)
Metals	32.1 (2)	42.0 (8)

[a] The numbers in parentheses are for the highest resolution shell.
[b] r.m.s.d., root mean square deviation.
[c] The number of atoms is listed in the parentheses.

cryosolvent was prepared by mixing 20% glycerol with the well buffer. Diffraction data of PDE5A1-IBMX were collected on beamline X12C at National Synchrotron Light Source (Table I). It has the space group P3$_1$21 with cell dimensions of $a = b = 74.5$, and $c = 130.1$ Å. All data were processed by program HKL (37).

Structure Determination—The PDE4D2 tetramer from the PDE4D2-rolipram structure (33) was directly applied to solve the structure of PDE4D2-IBMX, and the orientation of the tetramer was optimized by rigid body refinement of CNS (38). The structure of PDE5A1-IBMX was solved by molecular replacement program AMoRe (39), using the catalytic domain of PDE4D2 as the initial model and a data set collected on Raxis IV^{++} to 2.5-Å resolution. The translation search yielded a correlation coefficient of 0.182 and R-factor of 0.526 for 3247 reflections between 4 and 8 Å resolution. The amino acid differences between PDE5A1 and PDE4D2 were replaced, and the atomic model was rebuilt by program O (40) against the electron density map that was improved by the density modification package of CCP4 (41). The structure was refined by CNS (Table I). The coordinates have been deposited in the Protein Data Bank (accession codes 1RKO and 1RKP).

RESULTS AND DISCUSSION

Overall Structures—The crystallographic asymmetric unit of PDE4D2 in complex with IBMX contains four catalytic domains (residues 79–438) that form a tetramer. The monomer of PDE4D2-IBMX consists of 16 helices (Fig. 1) that fold into three subdomains as described previously in the structures of PDE4B (31) and PDE4D2-rolipram (33). The catalytic domain of PDE5A1 (residues 535–860) contains 16 helices and has the same folding topology as that of PDE4D2 (Fig. 1). The crystal of PDE5A1 contains one catalytic domain in the crystallographic asymmetric unit, which apparently exists as a monomer. This is consistent with the biochemical studies that the monomeric fragment of bovine PDE5A (residues 508–865) has similar catalytic activity as the full-length PDE5A (36). The electron density showed that residue 778 of PDE5A1 is better modeled with leucine instead of isoleucine in the wild type PDE5A1 sequence. The interpretation of this observation is not clear, but it may be caused by spontaneous mutation during PCR.

The superposition of the catalytic domains of PDE5A1 over PDE4D2 showed an root mean square deviation of 1.5 Å for the Cα atoms of 257 superimposable residues. However, the root mean square deviation increases to 4.8 Å if the entire catalytic domain is compared (312 residues). Three regions show different tertiary structures and are not superimposable, in addition to residues 289–298 in PDE4D2, which become a short connec-

tion with deletion of 6 residues in PDE5A1. The N-terminal regions of residues 79–113 in PDE4D2 and 535–566 in PDE5A1 contain two helices but have a totally different three-dimensional arrangement. The region of residues 208–224 in PDE4D2 and 661–676 in PDE5A1, which is labeled as *H-loop* in Fig. 1, shows differences of over 7 Å for the Cα atom positions of two short helices H8 and H9. Besides, the H-loop of PDE5A1 is flexible, although traceable in electron density, as shown by an average B-factor of 71.8 Å^2 in comparison with 36.6 Å^2 for all atoms of the structure. The region of residues 341–364 in PDE4D2 or 787–812 in PDE5A1 (M-loop in Fig. 1) shows dramatic conformational differences. Nine residues 341–349 at the tail of helix H14 in PDE4D2 are unfolded into coil or random conformations in PDE5A1. Residues 793–807 in PDE5A1 are not traceable due to lack of electron density and presumably exist in random conformation, in contrast to the ordered conformations of the corresponding sequences in PDE4D2.

It is interesting to note that our structure of PDE5A1-IBMX shows some conformational differences from those of PDE5A in complex with the inhibitors such as sildenafil. Although the structure of PDE5A-sildenafil is not available for a detailed comparison, the paper by Sung *et al.* (35) reported that residues 665–675 of the H-loop are disordered, and the M-loop is ordered in the PDE5A-sildenafil structure. In contrast, our structure of PDE5A1-IBMX shows that the H-loop is traceable, but the M-loop is disordered. One possible interpretation of these differences may be that bindings of each of the different inhibitors selectively affect the conformations of these loops. Besides, we note that the catalytic activity of our recombinant fragment 535–860 of PDE5A1 (2 μmol/min/mg) is about 800 times higher than that of the fragment 537–860 for the PDE5A-sildenafil structure (0.0025 μmol/min/mg) (35). Nevertheless, the structural studies by the two groups imply that the conformational flexibility of H- and M-loops may play roles in inhibitor selectivity.

Metal Binding—Two metal-binding sites have been assigned in the crystal structures of PDE4B and PDE4D2 as follows: one is zinc and another is ambiguous (31, 33, 34). Two metal sites are also found in the structure of PDE5A1 and occupy the same location as in the PDE4 structures (Fig. 1). In the PDE5A1 structure, the strongest peak in the $2F_o - F_c$ map has about 10 times the background and is assigned as zinc, despite the fact that no zinc was added during expression, purification, and crystallization of PDE5A1. This site coordinates with His-617, His-653, Asp-654, Asp-764, and two bound water molecules. These six coordinations form an octahedron and are the same as in PDE4 (31, 33). The role of the equivalent residues His-607 and His-643 of bovine PDE5 in metal coordination was established by site-directed mutagenesis (42). The second metal ion forms an octahedron with Asp-654 and five bound water molecules and has the same coordinations as in PDE4D2. The second metal ion is assigned as magnesium in the crystal because 0.2 M MgSO$_4$ was used in crystallization. The crystallographic refinement showed that both metal ions have the B-factors comparable with the overall average B-factor of the protein atoms (Table I), in support of the assignment. However, the physiological metal ions await to be identified. Biochemical studies have suggested that zinc is the optimal divalent cation for supporting catalysis in PDE5A1 (43).

IBMX Binding—The electron density maps that were calculated from the PDE4D2 and PDE5A1 structures without IBMXs show that IBMX binds to a subpocket of the active site of PDEs (Fig. 2). The majority of IBMX-binding residues are conserved between PDE4 and PDE5. Thus, the xanthine ring of IBMX stacks against Phe-372 of PDE4D2 or Phe-820 of
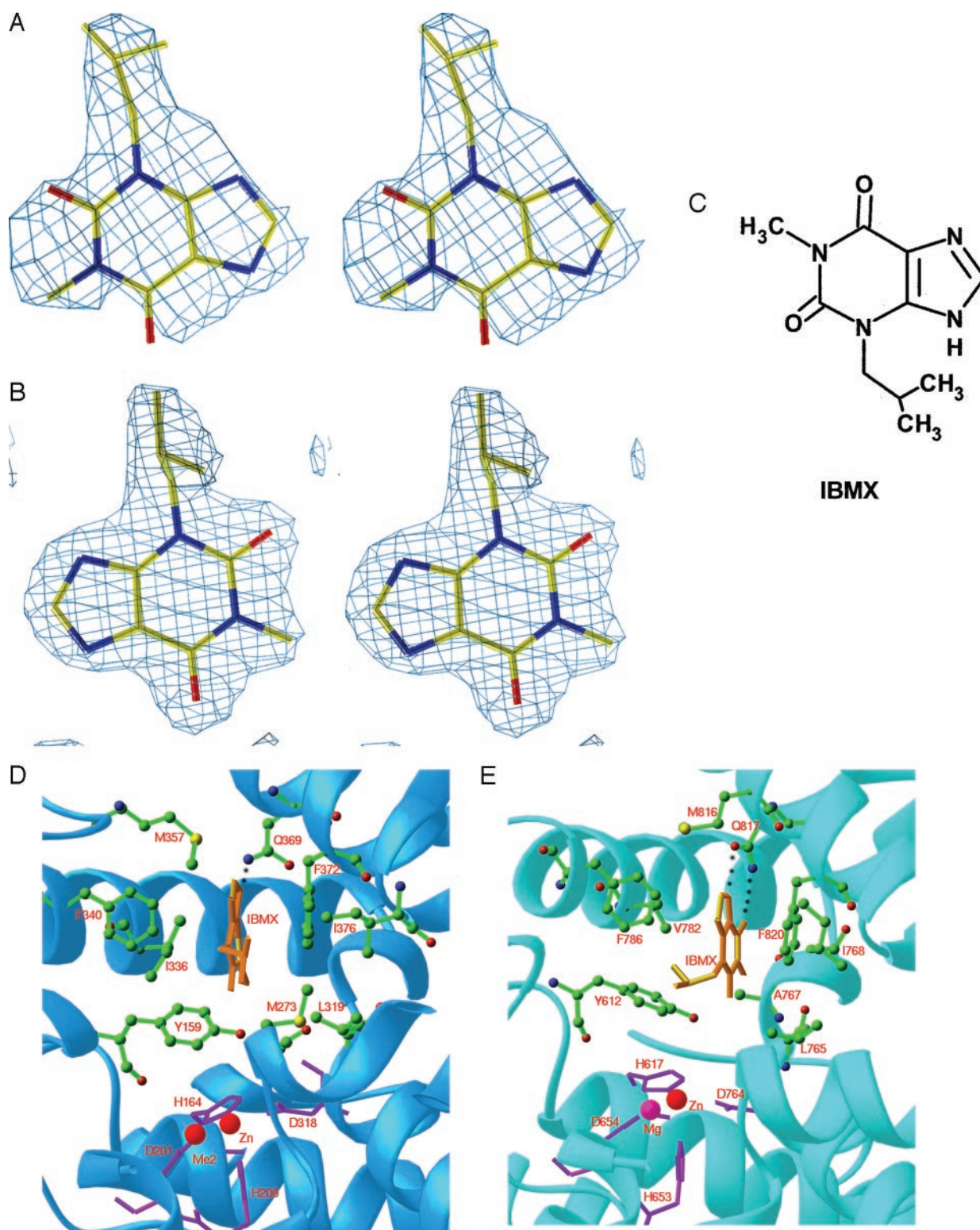
FIG. 2. **IBMX binding.** Stereoview of the electron density for IBMX bound to PDE4D2 (*A*) and PDE5A1 (*B*). The $2F_o - F_c$ maps were calculated from the structures omitted IBMX and contoured at 1.5σ for PDE4D2 and 2.0σ for PDE5A1. *C*, chemical structure of IBMX. *D*, IBMX binding to the active site of PDE4D2. The xanthine group stacks against Phe-372 and forms hydrogen bond with Gln-369 (*dotted lines*). *E*, IBMX binding to the active site of PDE5A1.

PDE5A1 on one side and contacts hydrophobic residues Ile-336 and Phe-340 of PDE4D2 or Val-782 and Phe-786 of PDE5A1 on another side. IBMX forms a hydrogen bond with the side chain of Gln-369 in PDE4D2 or Gln-817 in PDE5A1, in addition to hydrophobic interactions with Leu-319 and Asn-321 of PDE4D2 or Leu-765 and Ala-767 of PDE5A1.

On the other hand, IBMX shows some distinct interactions in the two PDE structures. First, O-6 of IBMX forms a hydrogen bond with Nϵ-2 of Gln-817 in PDE5A1, but with a water molecule in PDE4D2. Second, the xanthine ring of IBMX shows a translational shift of about 2 Å when the protein structures of PDE4D2 and PDE5A1 are superimposed (Fig. 2). Third, the

isobutyl group of IBMX has different orientations in the two structures and interacts with different residues as follows: Phe-786 of PDE5A1 but Met-273 and Ile-376 of PDE4D2. Finally, IBMX shows unique interactions with Met-273 and Met-357 in PDE4D2 but with Ile-768 in PDE5A1.

At the protein level, the amide group of the Gln-817 side chain of PDE5A1 has an opposite orientation from that of Gln-369 of PDE4D2. The configuration of the side chain amide group of Gln-817 in PDE5A1 is apparently fixed by the hydrogen bond to the side chain of Gln-775 that in turn forms hydrogen bonds with Nϵ-1 of Trp-853 and the backbone carbonyl oxygen of Ala-767. However, the torsion angle for the amide side chain of Gln-369 in PDE4D2 is about 180º different from Gln-817 of PDE5A1. This configuration of the Gln-369 side chain appears to be essential for formation of hydrogen bonds with Oh1 of Tyr-329 and N-7 of IBMX and is also observed in the structure of PDE4D2-rolipram (33).

The conservation of the majority residues for the IBMX binding agrees in general with the biochemical studies that IBMX is a nonselective inhibitor for various PDEs (44). The extra hydrogen bond between O-6 of IBMX and Gln-817 of PDE5A1 may account for the slightly higher potency of IBMX in PDE5 ($IC_{50} = 10\ \mu M$) (45) than that in PDE4 ($IC_{50} = 31\ \mu M$) (46). We speculate that four residues of Ile-336, Phe-340, Gln-369, and Phe-372 of PDE4D2 or Val-782, Phe-786, Gln-817, and Phe-820 of PDE5A1 may define a subpocket for the common binding of nonselective inhibitors of most PDEs. However, it is not clear why IBMX shows significant variations on orientation in the structures of PDE4D2 and PDE5A1. One possible interpretation may be that the active sites in different PDE families possess the key conserved components for binding of the nonselective inhibitor IBMX but have slightly different shapes and sizes. The conformational variation of the active sites in different PDE families may thus require an adjustment of the IBMX orientation to make the best fit in each PDE family. In other words, the conformation of the active site is a determinant for binding of inhibitors.

Implication for Inhibitor Selectivity—Selective inhibitors of PDE families have been widely studied as therapeutic agents for various human diseases. Enhancement of selectivity is critical for reducing side effects of the drugs. The structure of PDE4D2 in complex with rolipram showed a good conservation of the most rolipram-binding residues, but a few of them mutate dramatically across PDE families (33). This suggests that variation of the active site residues may selectively distinguish inhibitors according to their chemical groups, and therefore the chemical nature of the active site residues may be a determinant for inhibitor selectivity.

On the other hand, structural comparison between PDE4 and PDE5 suggests that different shapes of the active sites may also be a determinant of inhibitor selectivity. The structure of PDE5 shows three regions having different conformations from PDE4. Whereas the N-terminal region of 79–113 of PDE4D2 is apparently too far to directly contribute to inhibitor selectivity, H-loop (residues 208–224 of PDE4D2 or 661–676 in PDE5A1) and M-loop (residues 341–364 in PDE4D2 or 787–812 in PDE5A1) are located near the active site. H-loop does not directly contact IBMX and the PDE4-selective inhibitor rolipram (33) but constitutes an edge of the active site. The different conformations of H-loops will make different shapes and sizes of the active sites in PDE4D2 and PDE5A1, thus impacting selective binding of inhibitors. Recent work on the structures of PDE5-sildenafil proposed that Tyr-664 in the H-loop is involved in interaction with sildenafil (35), supporting a role for the H-loop in selective binding of PDE5 inhibitors. On the other hand, Met-357 of the M-loop (residues 341–364) in PDE4D2

forms hydrophobic interactions with the cyclopentane ring of the PDE4-selective inhibitor rolipram (33), indicating its role in binding of the selective inhibitor. In contrast, the corresponding residues 787–812 of PDE5A1 show significantly different conformations: the unfolding of C-terminal end of helix H14 and disordered conformation of 793–807 in PDE5A1 (Fig. 1). Therefore, the M-loop would have different contact patterns when interacting with PDE5 inhibitors from the mode in PDE4. In summary, our structural study suggests that both the conformation of the active site and the chemical nature of the residues in contact with the inhibitors contribute to the selectivity.

REFERENCES

1. Antoni, F. (2000) *Front. Neuroendocrinol.* **21,** 103–132
2. Pelligrino, D. A., and Wang, Q. (1998) *Prog. Neurobiol.* **56,** 1–18
3. Carvajal, J. A., Germain, A. M., Huidobro-Toro, J. P., and Weiner, C. P. (2000) *J. Cell. Physiol.* **184,** 409–420
4. Lucas, K. A., Pitari, G. M., Kazerounian, S., Ruiz-Stewart, I., Park, J., Schulz, S., Chepenik, K. P., and Waldman, S. A. (2000) *Pharmacol. Rev.* **52,** 375–414
5. Klein, C. (2002) *Cell. Signal.* **14,** 493–498
6. Chin, K. V., Yang, W. L., Ravatn, R., Kita, T., Reitman, E., Vettori, D., Cvijic, M. E., Shin, M., and Iacono, L. (2002) *Ann. N. Y. Acad. Sci.* **968,** 49–64
7. Manganiello, V. C., Taira, M., Degerman, F., and Belfrage, P. (1995) *Cell. Signal.* **7,** 445–455
8. Müller, T., Engels, P., and Fozard, J. R. (1996) *Trends Pharmacol. Sci.* **17,** 294–298
9. Houslay, M. D., Sullivan, M., and Bolger, G. B. (1998) *Adv. Pharmacol.* **44,** 225–343
10. Houslay, M. D., and Adams, D. R. (2003) *Biochem. J.* **370,** 1–18
11. Torphy, T. J. (1998) *Am. J. Respir. Crit. Care Med.* **157,** 351–370
12. Corbin, J. D., and Francis, S. H. (1999) *J. Biol. Chem.* **274,** 13729–13732
13. Soderling, S. H., and Beavo, J. A. (2000) *Curr. Opin. Cell Biol.* **12,** 174–179
14. Francis, S. H., Turko, I. V., and Corbin, J. D. (2001) *Prog. Nucleic Acids Res. Mol. Biol.* **65,** 1–52
15. Conti, M., Richter, W., Mehats, C., Livera, G., Park, J. Y., and Jin, C. (2003) *J. Biol. Chem.* **278,** 5493–5496
16. Mehats, C., Andersen, C. B., Filopanti, M., Jin, S. L., and Conti, M. (2002) *Trends Endocrinol. Metab.* **13,** 29–35
17. Manganiello, V. C., Murata, T., Taira, M., Belfrage, P., and Degerman, F. (1995) *Arch. Biochem. Biophys.* **322,** 1–13
18. Degerman, E., Belfragem, P., and Manganiello, V. C. (1996) *Biochem. Soc. Trans.* **24,** 1010–1013
19. Corbin, J. D., and Francis, S. H. (2002) *Int. J. Clin. Pract.* **56,** 453–459
20. Movsesian, M. A. (2000) *Exp. Opin. Investig. Drugs* **9,** 963–973
21. Truss, M. C., Stief, C. G., Uckert, S., Becker, A. J., Wafer, J., Schultheiss, D., and Jonas, U. (2001) *World J. Urol.* **19,** 344–350
22. Liu, Y., Shakur, Y., Yoshitake, M., and Kambayashi, J. J. (2001) *Cardiovasc. Drug Rev.* **19,** 369–386
23. Huang, Z., Ducharme, Y., MacDonald, D., and Robinchaud, A. (2001) *Curr. Opin. Chem. Biol.* **5,** 432–438
24. Rotella, D. P. (2002) *Nat. Rev. Drug Discovery* **1,** 674–682
25. Barnette, M. S. (1999) *Prog. Drug Res.* **53,** 193–229
26. Souness, J. E., Aldous, D., and Sargent, C. (2000) *Immunopharmacology* **47,** 127–162
27. Barnette, M. S., and Underwood, D. C. (2000) *Curr. Opin. Pulmonary Med.* **6,** 164–169
28. Piaz, V. D., and Giovannoni, P. (2000) *Eur. J. Med. Chem.* **35,** 463–480
29. Giembycz, M. A. (2002) *Monaldi Arch. Chest Dis.* **57,** 48–64
30. Sturton, G., and Fitzgerald, M. (2002) *Chest* **121,** S192–S196
31. Xu, R. X., Hassell, A. M., Vanderwall, D., Lambert, M. H., Holmes, W. D., Luther, M. A., Rocque, W. J., Milburn, M. V., Zhao, Y., Ke, H., and Nolte, R. T. (2000) *Science* **288,** 1822–1825
32. Lee, M. E., Markowitz, J., Lee, J. O., and Lee, H. (2002) *FEBS Lett.* **530,** 53–58
33. Huai, Q., Wang, H., Sun, Y., Kim, H. Y., Liu, Y., and Ke, H. (2003) *Structure* **11,** 865–873
34. Huai, Q., Colicelli, J., and Ke, H. (2003) *Biochemistry* **42,** 13200–13226
35. Sung, B. J., Hwang, K. Y., Jeon, Y. H., Lee, J. I., Heo, Y. S., Kim, J. H., Moon, J., Yoon, J. M., Hyun, Y. L., Kim, E., Eum, S. J., Park, S. Y., Lee, J. O., Lee, T. G., Ro, S., and Cho, J. M. (2003) *Nature* **425,** 98–102
36. Fink, T. L., Francis, H., Beasley, A., Grimes, K. A., and Corbin, J. D. (1999) *J. Biol. Chem.* **274,** 24613–24620
37. Otwinowski, Z., and Minor, W. (1997) *Methods Enzymol.* **276,** 307–326
38. Brünger, A. T., Adams, P. D., Clore, G. M., DeLano, W. L., Gros, P., Grosse-Kunstleve, R. W., Jiang, J. S., Kuszewski, J., Nilges, M., Pannu, N. S., Read, R. J., Rice, L. M., Simonson, T., and Warren, G. L. (1998) *Acta Crystallogr. Sect. D Biol. Crystallogr.* **54,** 905–921
39. Navaza, J., and Saludjian, P. (1997) *Methods Enzymol.* **276,** 581–594
40. Jones, T. A., Zou, J. Y., Cowan, S. W., and Kjeldgaard, M. (1991) *Acta Crystallogr. Sect. A* **47,** 110–119
41. Collaborative Computational Project, Number 4 (1994) *Acta Crystallogr. Sect. D Biol. Crystallogr.* **50,** 760–763
42. Francis, S. H., Turko, I. V. Grimes, K. A., and Corbin, J. D. (2000) *Biochemistry*

39, 9591–9596

43. Francis, S. H., Colbran, J. L., McAllister-Lucas, L. M., and Corbin, J. D. (1994) *J. Biol. Chem.* **269,** 22477–22480

44. Beavo, J. A., Rogers, N. L., Crofford, O. B., Hardman, J. G., Sutherland, E. W., and Newman, E. V. (1970) *Mol. Pharmacol.* **6,** 597–603

45. Sekhar, K. R., Grondin, P., Francis, S. H., and Corbin, J. D. (1996) in *Phosphodiesterase Inhibitors* (Schudt, C., Dent, G., and Rabe, K. F., eds) pp. 135–146, Academic Press, New York

46. Alvarez, R., Daniels, D. V., Shelton, E. R., Baecker, P. A., Fong, T. A. T., Devens, B., Wilhelm, R., and Eglen, R. M. (1996) in *Phosphodiesterase Inhibitors* (Schudt, C., Dent, G., and Rabe, K. F., eds) pp. 161–171, Academic Press, New York